The Dependence of Electronic Structure and Optical Absorption Coefficient on the Size and Mass of the Wurtzite ZnS Quantum Dot

M. K. Shamer^{a, *} and H. K. Fadel^{a, **}

^aDepartment of Physics, College of Education for Pure Sciences, University of Basra, Basra 42002 Iraq
*e-mail: musashamer@yahoo.com
**e-mail: haider.qassim@uobasrah.edu.iq
Received March 15, 2020; revised April 22, 2020; accepted April 25, 2020

Abstract—The density functional theory is used to analyze the electronic band structures of various atoms and molecules. The effect of quantum confinement on the electronic and exciton band structures is taken into account, which optical properties are insensitive to light polarization. The effective mass approximation, the valance band degeneracy, and the reduced effective mass in the parallel and perpendicular directions of the electrons and holes are also taken into account. The dispersion relation, quantum confinement effects, joint density of states, refractive index, and absorption coefficient are calculated and discussed, which gives good agreement with the theoretical calculations and experimental measurements.

Keywords: quantum dot, effective mass, quantum confinement, optical absorption

DOI: 10.1134/S1027451020060439

INTRODUCTION

The potential energy of an electron in a crystal is known to be periodic in space, but the most important is the energy spectrum, which is divided into allowed and forbidden energy bands. For allowed bands, the energy spectrum is determined by the dependence of energy on the quasi-momentum, E(p). A certain number of allowed bands with the lowest energy are completely filled with electrons in insulators and semiconductors at zero temperature (according to the Pauli principle), while bands with a higher energy are empty. In the case of semiconductors, the energy band gap varies from zero (the so-called gapless semiconductor, such as HgTe) to 3 eV. The number of free carriers (electrons in the conduction band or holes in the valence band), which is an important property of semiconductors, is always small compared to the number of atoms. Carriers are formed either by doping or by thermal excitation, in which the number of electrons is equal to the number of holes. In the case when the carrier concentration never exceeds 10^{20} cm⁻³, the number of states per 1 cm⁻³ in this band is about 10²², i.e., typical electrons occupy only a very small fraction of the valence band. In the center of the Brillouin zone (p = 0, as in the case of GaAs) and for a small momentum p, the function E(p) should be parabolic.

The electronic bands of semiconductors (wurtzite type) near the center of the Brillouin zone (in the directions parallel and perpendicular to the c^* -axis of the reciprocal space) are defined as [1]:

$$E_e = E_g + \frac{\hbar^2 k^2}{2m_e^*},$$
 (1)

$$E_A(HH) = -\frac{\hbar^2 k^2}{2m_{HH}^*},$$
 (2)

$$E_B(LH) = -\frac{\hbar^2 k^2}{2m_{LH}^*} - \Delta_{CF}, \qquad (3)$$

$$E_C(SO) = -\frac{\hbar^2 k^2}{2m_{SO}^*} - \Delta_{CF} - \Delta_{SO}, \tag{4}$$

because the valence bands are split into three subbands in the center of the Brillouin zone due to the $\Delta_{\rm CF}$ crystal field and $\Delta_{\rm SO}$ spin orbit interaction. The effective mass may be anisotropic, i.e., have different values for different directions in the crystal, m_e^* is the electron effective mass, and $m_{\rm HH}^*$, $m_{\rm LH}^*$, $m_{\rm SO}^*$ are the hole effective masses (heavy-hole (HH), light-hole (LH), and split-off (SO) bands). From the above equations we obtain the general expression for the effective mass [1]:

$$m^* = \hbar^2 \left(\frac{d^2 E(k)}{dk^2} \right)^{-1}.$$
 (5)

EFFECTIVE MASS APPROXIMATION

Using the principles of quantum mechanics for a particle in a potential box and the effective masses of electron and holes in terms of kinetic energy, by means of effective mass approximation we can calculate the energy band gap depending on the size of the quantum dot [2]. The effective mass approximation is a single-

particle Hamiltonian with a dispersion relation of the bulk band near the minimum and maximum points. A.L. Efros calculated the electronic structure of quantum dots using a very simple parabolic approximation of the effective mass and a free particle with mass m_0 inside a spherical potential well of radius R [3]:

$$V(\mathbf{r}) = \begin{cases} 0, & |r| < R \\ \infty, & |r| \ge R \end{cases}$$
 (6)

The Schrödinger equation for the particle in a spherical well with infinite potential depth can be written as follows:

$$\left(-\frac{\hbar^2}{2m_0}\nabla^2(\mathbf{r}) + V(\mathbf{r})\right)\Psi(\mathbf{r}) = E\Psi(\mathbf{r}). \tag{7}$$

Through the solution of the Eq. (7) in the spherical coordinates, the wave function takes the form:

$$\Psi_{nlm(r,\theta,\phi)} = CY_l^m(\theta,\phi) \frac{j_l(k_{n,l},r)}{r}, \tag{8}$$

where C is the normalization constant, $Y_l^m(\theta, \phi)$ is the spherical harmonic part, $j_l(k_{n,l}, r)$ is the spherical Bessel function of the lth order, $k_{n,l} = \phi_{nl}/R$ and ϕ_{nl} are the nth zeros of $j_l(k_{n,l}, r)$. Therefore, the energy of a free particle in spherical well is defined as:

$$E_{nl} = \frac{\hbar^2 k_{nl}^2}{2m_0} = \frac{\hbar^2 \phi_{nl}^2}{2m_0 R^2}$$
 (9)

This is the kinetic energy of a free particle and it is proportional to $1/R^2$, i.e., the quantized energy strongly depends on the size.

A free particle can be replaced by an electron or a hole and a spherical potential well can be replaced by a spherical quantum dot of radius R, so the quantized energy of the electron and hole can be estimated using the Eq. (9). The Coulomb interaction between an electron and a hole will not be ignored, except for the lowest electronic state of the quantum dot (n = 1, l = m = 0). The band gap of a quantum dot, E_{gOD} , is written as [4]:

$$E_{gQD} = E_g + \frac{\hbar^2 \pi^2}{2R^2} \left(\frac{1}{m_e^*} + \frac{1}{m_H^*} \right)$$

$$- \frac{1.786e^2}{4\pi\epsilon R} - 0.248 E_{Ry}^*.$$
(10)

The effective mass approximation assumes that the effective masses of carriers in quantum dot are the same in a bulk semiconductor, ϵ is the dielectric constant.

The additional energy due to the confinement is presented in the second term of the Eq. (10). The third term is the energy of the Coulomb interaction of excitons (often neglected). The last term, independent of radius, comes from the effect of spatial correlation and is advantageous only in the case of semiconductor materials with low dielectric constant; $E_{\rm Ry}^*$ refers to the effective Rydberg energy, which is determined by [5]:

$$E_{\text{Ry}}^* = \frac{e^4}{2\epsilon^2 \hbar^2} \left(\frac{1}{m_e^*} + \frac{1}{m_h^*} \right). \tag{11}$$

Equation (10) clearly shows that a decrease in the quantum dot size leads to an increase in the particle energy, which causes the absorption of light at shorter wavelengths.

The effective mass approximation was not successful for the smallest quantum dot size, because an extremely simplified description of the crystal potential taken as a spherical well with an infinitely high potential at the interface was used. Another problem is that the effective masses were assumed to be constant, but this is correct only when working with electronic states near the band edge [6]. Therefore, the effective mass approximation is applicable to relatively large quantum dots, whose intrinsic properties exceed the surface properties.

The data obtained in the effective mass approximation were compared with the experimental results [7– 9]. The comparison shows that in the range of nanoparticle sizes of 2.5–4 nm, the band gap increases at small sizes, and this agrees with the experimental results; the growth rate increases with the size of the nanoparticle, which leads to a huge difference between numerical and experimental results. The reasons for the disagreement are associated with the choice of masses (electron and hole), which are suitable only for bulk substances. In addition, the effective mass includes all existing interactions on an excited electron: therefore, a decrease in the particle diameter leads to a change in the effective mass. Hence, there is agreement between theory and experiment, since the changes for nanoparticles with a diameter of more than 2.5 nm are insignificant, the differences will appear for smaller particles.

The effective mass approximation cannot predict how the effective mass changes, and it cannot be used for low-dimension systems. There is another method suitable for calculating the variation of the effective mass, and also for determining the variation of the energy gap, this is the density functional approximation.

DENSITY FUNCTIONAL THEORY

Density functional theory (DFT) is a technique in quantum mechanics that is used to analyze electronic structures of various atoms and molecules. It allows determining the properties of the system using the spatial dependence of the electron density. Using DFT gives a set of single-particle equations (similar to Hartree—Fock equations), however the simplified DFT is a more accurate procedure for solids. It focuses on a simple scalar charge density field instead of a complex many-body wave function. The Schrödinger equation is derived to precisely determine the ground state charge density as a function of external potential. DFT is useful in many quantum molecular applications that involve quantum dots. For example, it can be used for structural analysis of a model of quantum dots of var-

Table 1. Calculation of ΔE_g and M_{eff} depending on quantum dot diameter

Diameter, nm	ΔE_g , eV	$M_{ m eff}$
Bulk	0	$0.21m_0$
1.47	0.81	$0.46m_0$
1.14	1.15	$0.57m_0$
0.73	1.52	$0.97m_0$
0.47	3.08	$1.3m_0$

ious materials [10-12]. It can also be applied to evaluate the use of quantum dots in colloidal charge transfer and nanoscale devices such as nanowires [13, 14].

It is possible to construct a relationship between the energy and the density of states for each quantum dot, as well as for the bulk according to the DFT. Hence, the energy gap of a quantum dot differs from that of bulk. From this calculation, for different diameters of quantum dots, we can estimate the relationship between the energy gap and the quantum dot diameter, as shown in [9], where the density of states calculated for the ZnS (wurtzite) nanoparticle and its bulk. Our comparison focused on finding the difference in energy gap from Eq. (10) and then finding the reduced effective masses for the electron—hole pair as shown in Table 1. It can be seen the energy gap difference and the decrease in effective masses increase with decreasing diameter. By plotting the reduced effective mass versus diameter and taking the best fit of the extracted data from the resulting curve, the following equation can be obtained:

$$\frac{M_{\text{eff}}}{m_0} = 0.21 + 2.39 \exp\left(-\frac{R}{5.59}\right). \tag{12}$$

The use of Eq. (12) does not give a difference between theoretical and experimental results for particles with a diameter less than 2.5 nm, which is in good agreement with [9].

OPTICAL ABSORPTION COEFFICIENT

The optical absorption spectrum plays an important role in many optoelectronic devices. The optical response of a semiconductor is characterized by the optical absorption coefficient, $\alpha(\omega)$, which is proportional to the number of optical transitions per unit volume and time. For quantum dots, that coefficient takes the following form [15–17]:

$$\alpha(\omega) = \frac{1}{V} \frac{4\pi^2 e^2}{m_e^2 \epsilon_0 \omega n_r c} |M_{cv}|^2 JDoS^{0D}, \qquad (13)$$

where M_{cv} is the momentum matrix element between the valence and conduction bands, JDoS is the joint density of states. The absorption coefficient $\alpha(\omega)$ increases with decreasing volume V of the quantum dot. The coefficient $\alpha(\omega)$ is also proportional to the joint density of states described by the following expression [18]:

$$JDoS^{0D} = 2\delta(E - E_{\sigma OD}), \tag{14}$$

the square of the absolute value of the momentum matrix element is specified in [16, 19]:

$$|M_{cv}|^2 = \frac{3m_0^2 E_{gQD} \left(E_{gQD} + \Delta_{SO} \right)}{2 \left(3E_{gQD} + 2\Delta_{SO} \right)} \left(\frac{1}{m_e^*} - \frac{1}{m_0} \right),$$
 (15)

 n_r represents the refractive index, which is related to the energy band gap. Moreover, the dielectric constant ϵ depends on the refractive index of the materials, which can be calculated as [20]:

$$n_r = \sqrt{\epsilon}. \tag{16}$$

There are many forms of the relationship between the energy gap E_g and refractive index n_r , which are widely used to calculate the refractive index of different group of semiconductors. Ravindra et al. proposed an expression for the refractive indices for semiconductors [21, 22]:

$$n_r = 4.084 + \beta, \ \beta = -0.62 \text{ eV}^{-1}.$$
 (17)

RESULTS AND DISCUSSION

In our calculations, we used the data in accordance with the local density approximation in the parallel (\parallel) and perpendicular (\perp) directions (Table 2). We used Eqs. (1)–(4) to construct an electronic band structure for a bulk semiconductor ZnS around the first Brillouin zone. The conduction band is a twofold degenerate band at k=0 due to spin, and it is well described by the effective mass approximation, while the valence band is six-fold degenerate, which is partly lifted by the spin-orbit coupling (Fig. 1). The valence bands are classified according to the total angular momentum J (J represents the sum of the orbital angular momentum and spin angular momentum).

Figure 2 shows the size dependence of the confinement energies calculated uding the Eq. (9). It is seen that a decrease in the quantum dot radius leads to a level shift. Moreover, these shifts largely depend on the effective masses of the carriers. The more the mass, the less the displacement. We can obtain a reduction in effective mass variation in the same way

Table 2. The effective masses (for electron, holes) and energies [24]

$m_e^{*\parallel}$	$m_e^{*\perp}$	$m_{ m HH}^{*\parallel}$	$m_{ m HH}^{*\perp}$	$m_{ m HL}^{*\parallel}$	$m_{ m HL}^{*\perp}$	$m_{\mathrm{SO}}^{*\parallel}$	$m_{\mathrm{SO}}^{*\perp}$	E_g , eV	Δ_{CF} , eV	Δ_{SO} , eV
0.144	0.153	1.746	3.838	0.756	0.180	0.183	0.337	1.9681	0.0518	0.0269

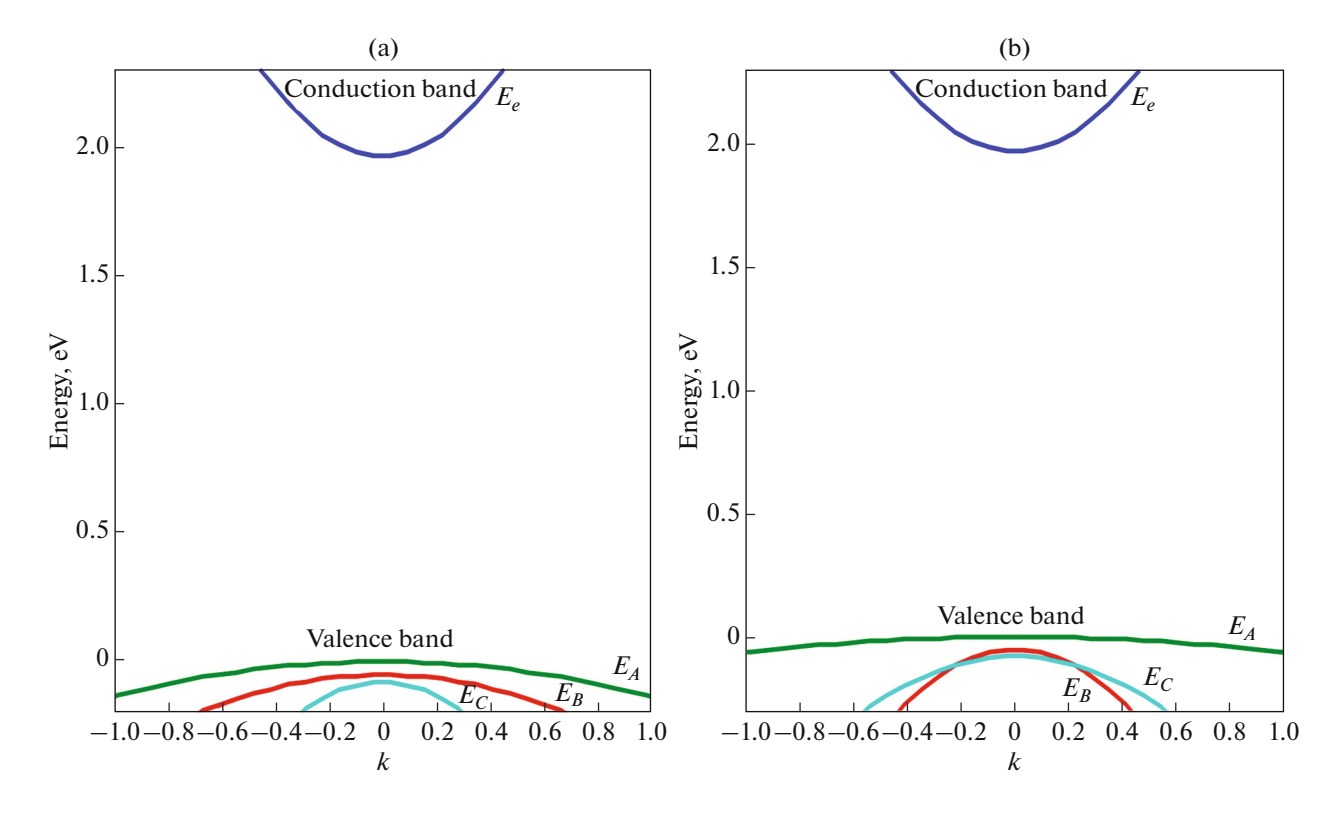


Fig. 1. Electronic band structure around the center of the Brillouin zone for bulk ZnS in directions (a) parallel and (b) perpendicular to the c^* -axis of the reciprocal space.

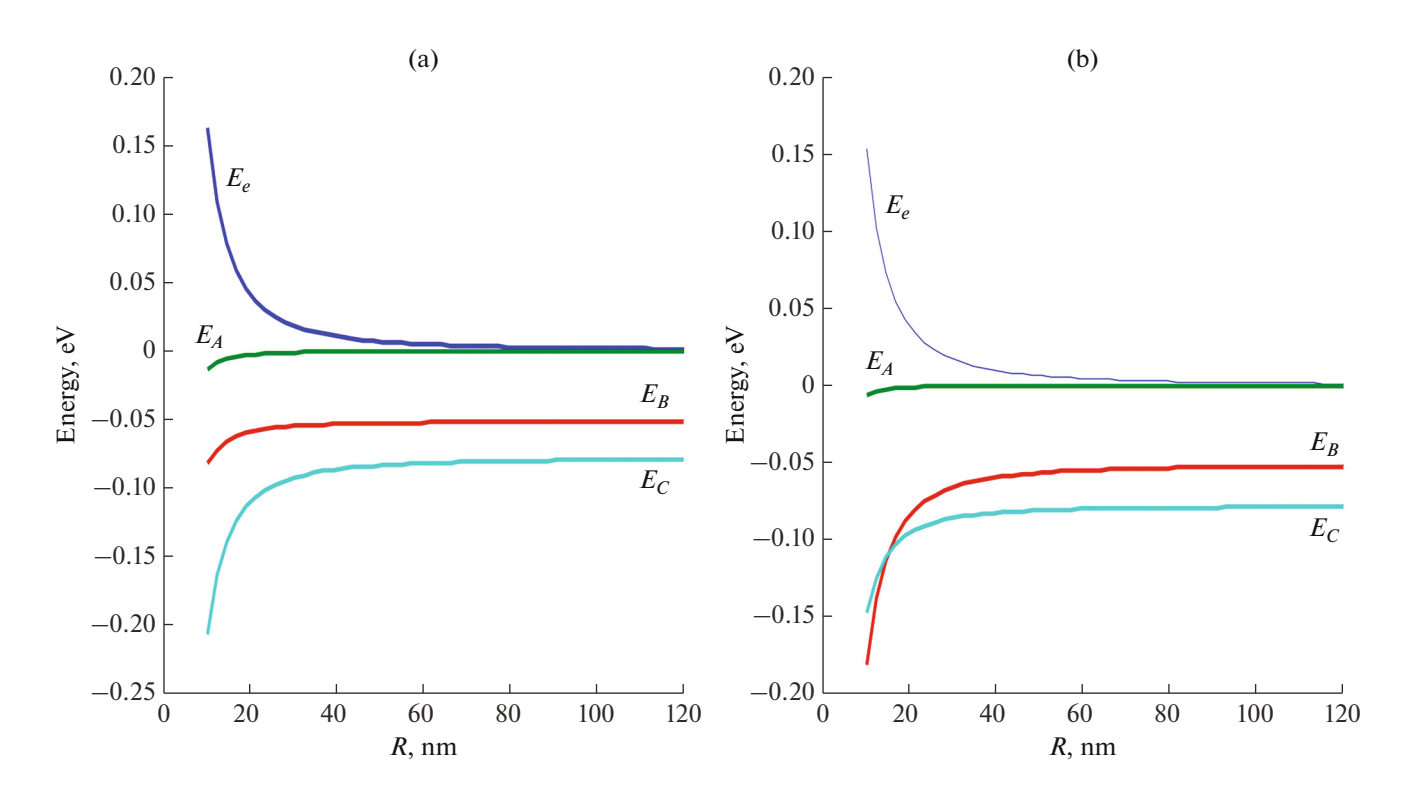


Fig. 2. The lowest quantum confinement levels of the valence subbands of electrons (e) and holes (HH (A), LH (B), and SO (C)) as a function of the size of a spherical wurtzite quantum dot in directions (a) parallel and (b) perpendicular to the c*-axis of the reciprocal space.

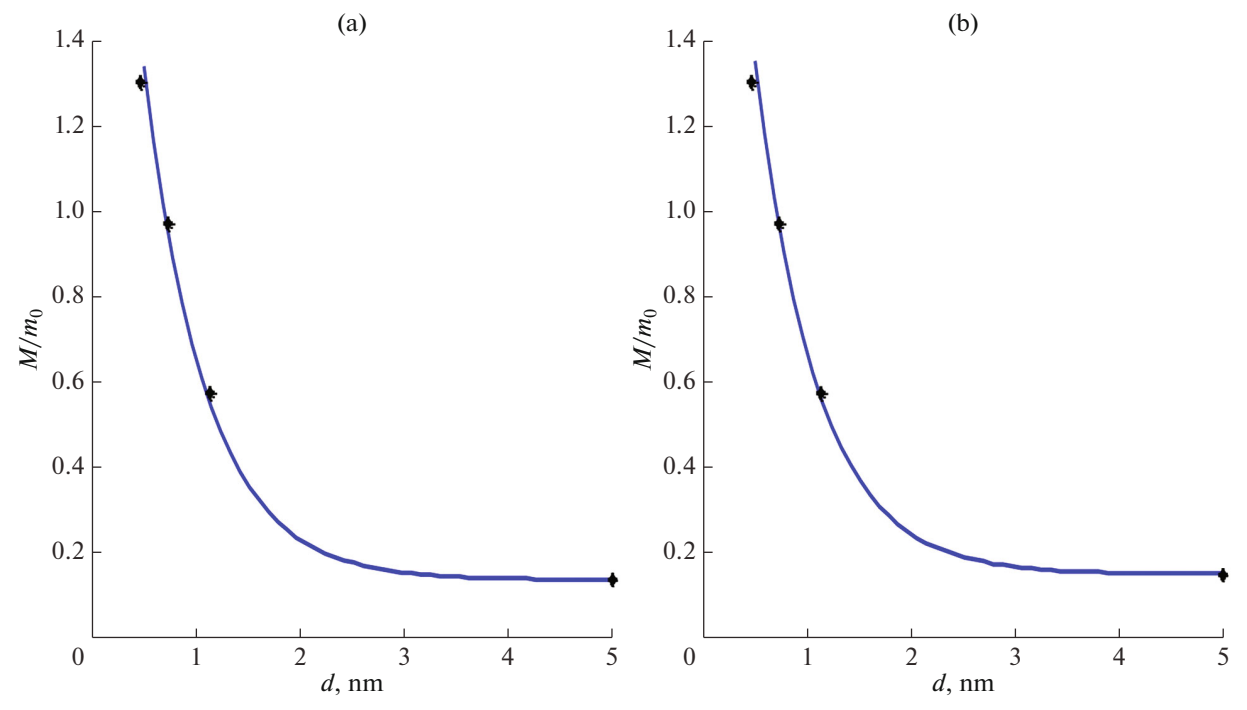


Fig. 3. Effective mass variation as a function of the ZnS quantum dot diameter obtained using the density functional theory (symbols) and Eq. (18) (solid line) for (a) parallel and (b) perpendicular directions.

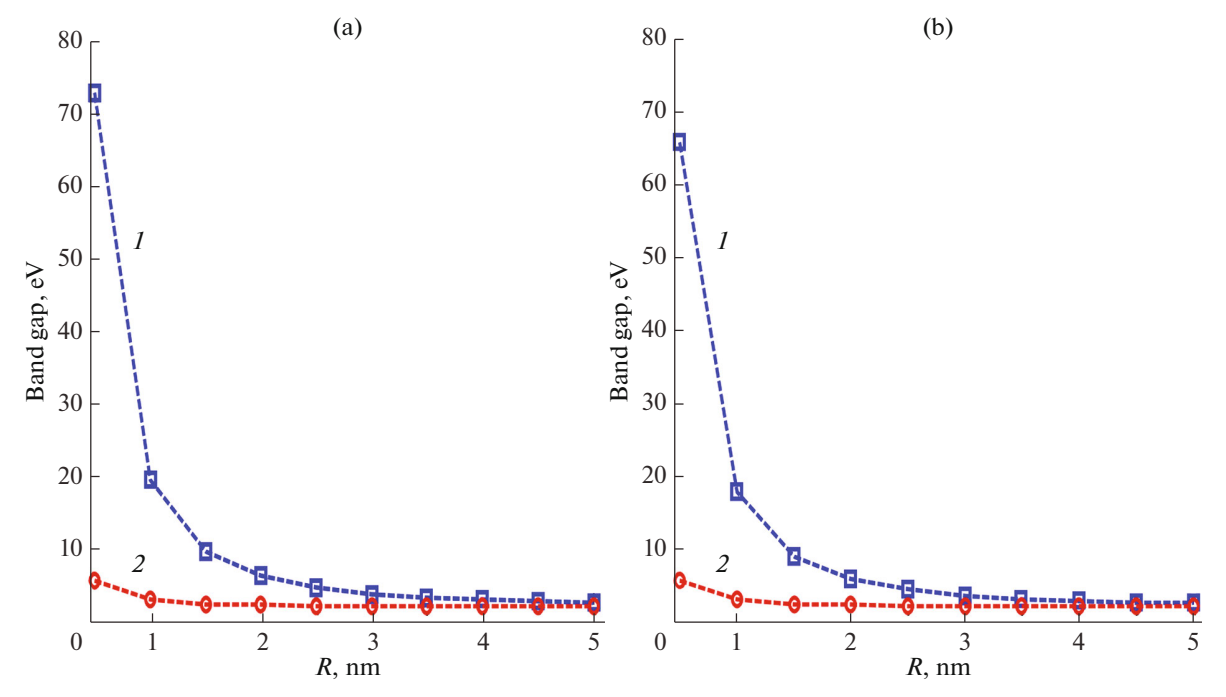


Fig. 4. Dependence of the band gap energy on the radius of a spherical quantum dot obtained using the (line *I*) effective mass approximation and (line *2*) Eq. (18) for (a) parallel and (b) perpendicular directions.

for parallel and perpendicular directions, as shown below:

$$M = Am_0 + 2.8m_0 \exp(-R/5.59), \tag{18}$$

where A = 0.133 for parallel and 0.1471 for perpendicular directions, respectively.

Figure 3 shows our results for the effective mass variation depending on the diameter of the ZnS quantum dot, obtained using the effective mass approximation and Eq. (18) for parallel and perpendicular directions, as well using the density functional theory and Eq. (18). The energy band gap E_{gQD} increases with

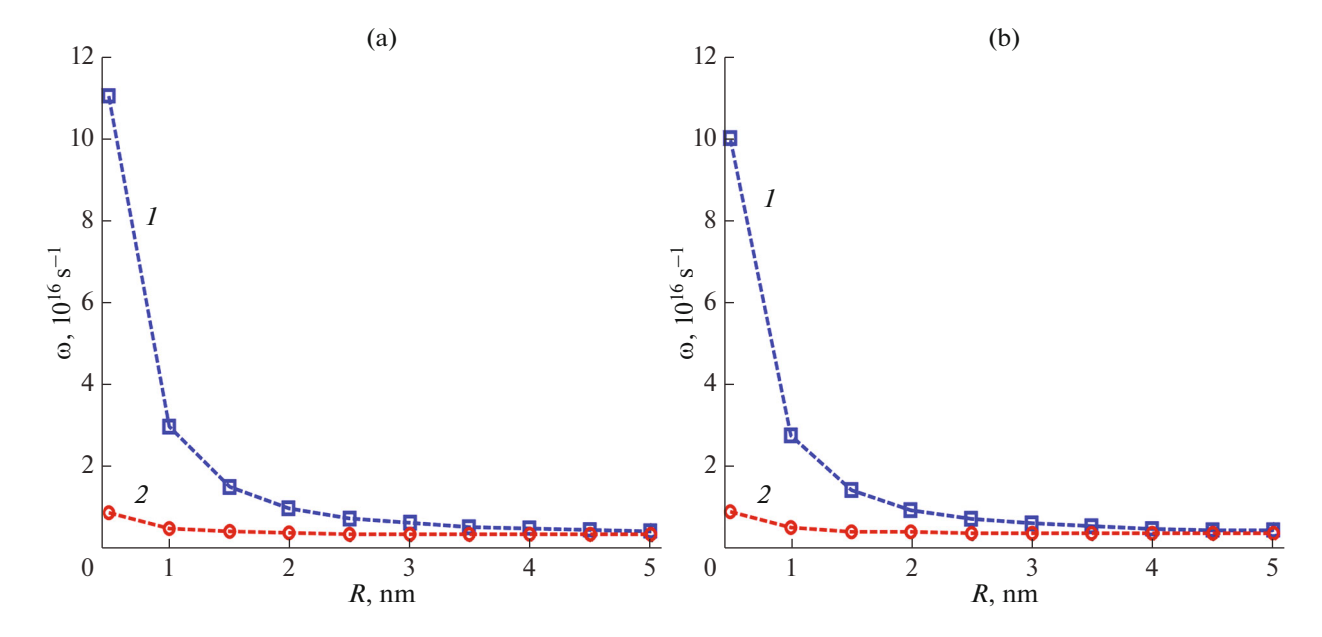


Fig. 5. Dependence of the angular frequency on the radius of a spherical quantum dot obtained using the (line *I*) effective mass approximation and (line *2*) Eq. (18) for (a) parallel and (b) perpendicular directions.

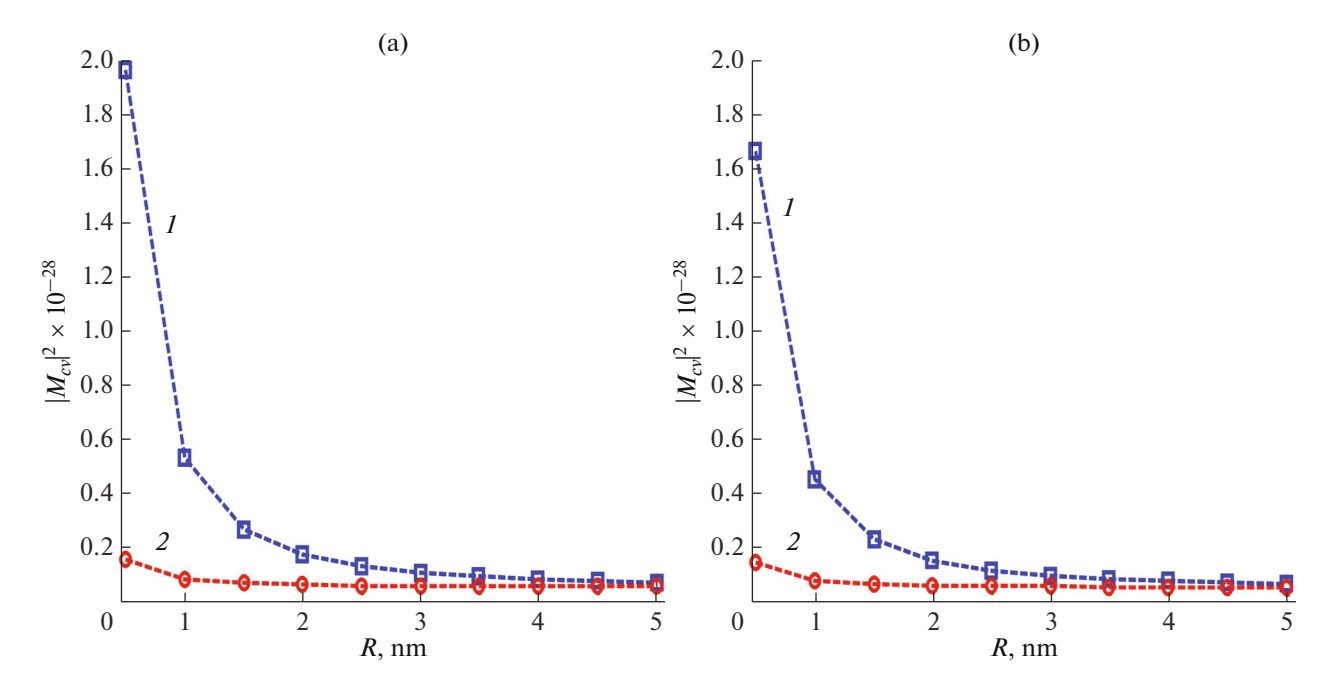


Fig. 6. Dependence of $|M_{cv}|^2$ on the radius of a spherical quantum dot obtained using the (line 1) effective mass approximation and (line 2) Eq. (18) for (a) parallel and (b) perpendicular directions.

decreasing radius of the spherical quantum dot (Fig. 4); there is a difference in the band gap energies. The gap energy obtained using the effective mass approximation is greater than that calculated using the Eq. (18). Figures 5, 6 show the behavior of the angular frequency and the square of the absolute value of the momentum matrix element $|M_{cv}|^2$ depending on the radius of the quantum dot. It is clear that the use of Eq. (18) gives a slightly decreasing curve, different

from the curve obtained in the effective mass approximation, especially for smaller quantum dot radius (less than 3 nm).

Figure 7 shows the change in the joint density of states with an energy gap. The behavior corresponds to the Dirac delta function and is dominant in the energy range of the band gap (in the effective mass approximation, the range is 0-80 eV for the parallel direction and 0-70 eV for the perpendicular direction), while in

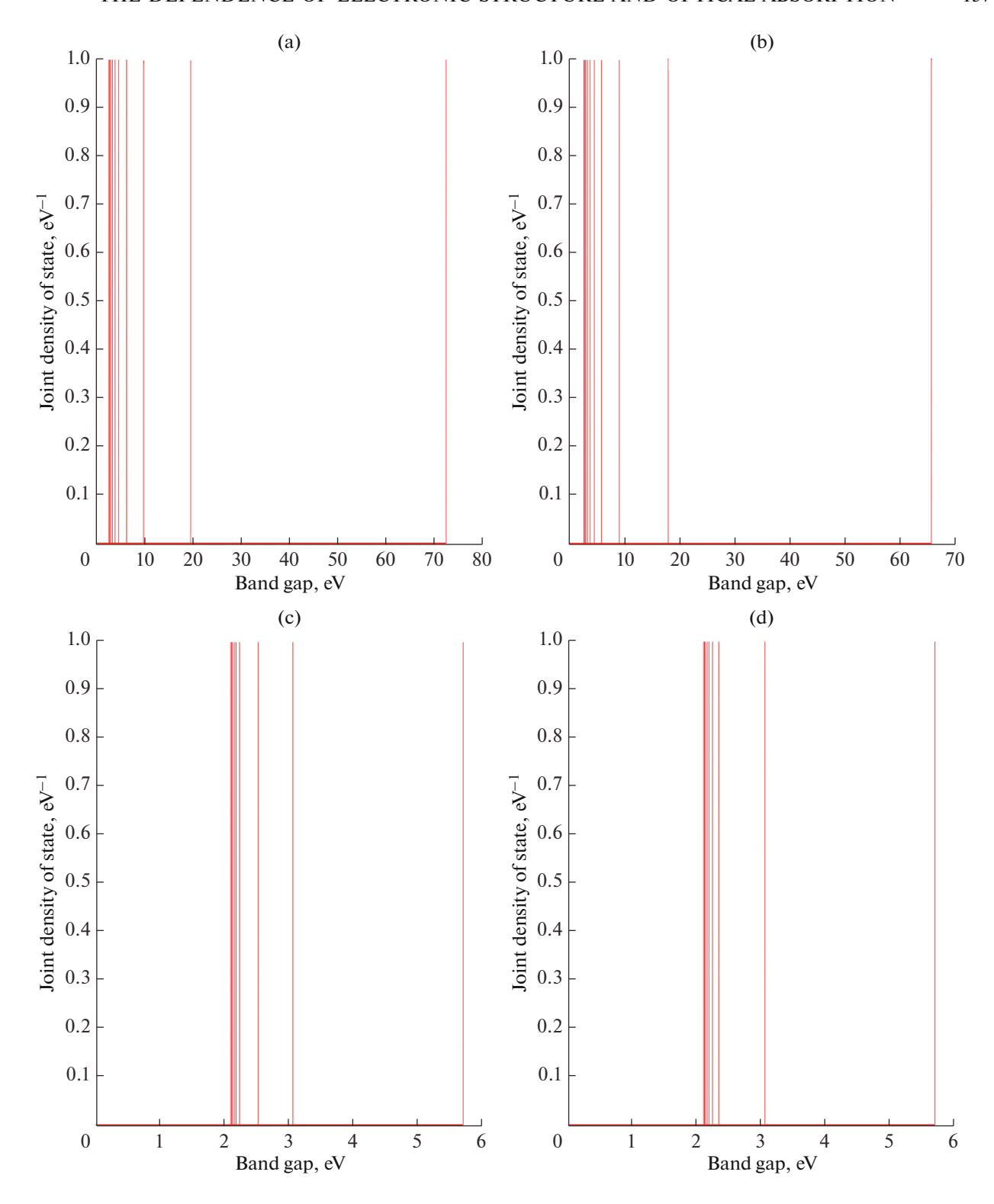


Fig. 7. Joint density of states as a function of the band gap for a single quantum state of a spherical ZnS quantum dot obtained using the (a, b) effective mass approximation and (c, d) Eq. (18) for (a, c) parallel and (b, d) perpendicular directions.

our calculations the *JDoS* shows the same behavior in the range 0–6 eV for both directions. Figure 8 shows the variation of the absorption coefficient with the energy gap. For parallel and perpendicular directions,

we obtain the same values of the absorption coefficient corresponding to different energies, which we obtained using the effective mass approximation and the Eq. (18). There is a difference between results for

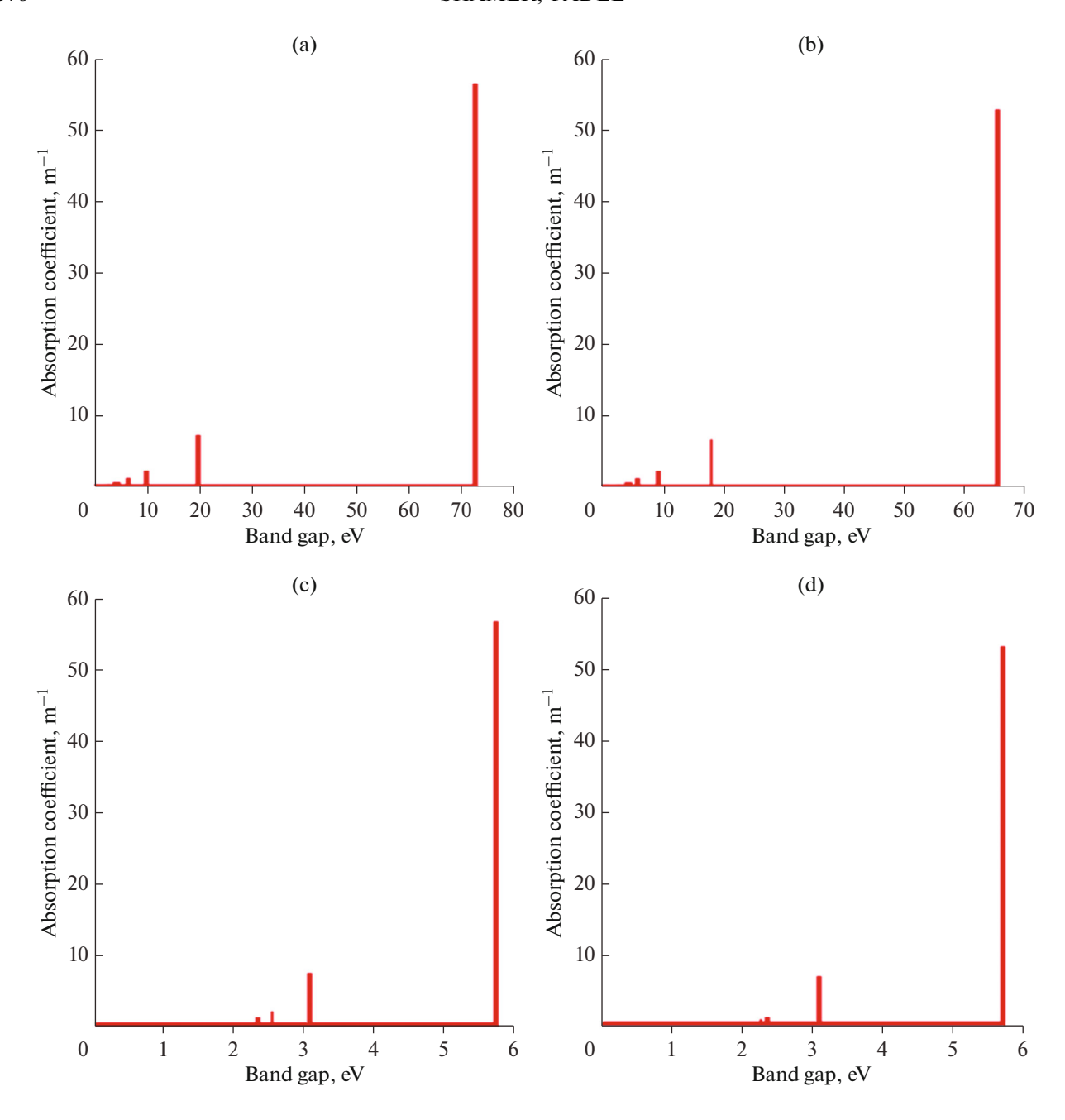


Fig. 8. Absorption coefficient as a function of the band gap for a single quantum state of a spherical ZnS quantum dot obtained using the (a, b) effective mass approximation and (c, d) Eq. (18) for (a, c) parallel and (b, d) perpendicular directions.

the two directions that give the highest absorption coefficient, because the band gap ranges are different between these two techniques when calculating the angular frequency and the moment matrix elements. A larger absorption coefficient corresponds to a larger energy gap, which in itself corresponds to a smaller quantum dot size (strong confinement).

CONCLUSIONS

The effect of quantum confinement on the band gap and absorption coefficient for a spherical quantum

dot of wurtzite ZnS is studied. The effective masses of charge carriers, the spherical conduction band and the threefold valence band (heavy-hole, light-hole and split-off) were taken into account. Quantum confinement causes the band gap to expand with decreasing quantum dot size (proportional to R^{-2}), while the material is still in the semiconductor range. According to the Bohr radius $r_{\rm B}$ and the quantum dot radius R, there are two regimes: the weak confinement regime $(r_{\rm B} < R)$ and the strong confinement $(r_{\rm B} > R)$ regime. The absorption edge of the large dot $(r_{\rm B} < R)$ is similar

to that of the bulk crystal. An increase in the energy gap leads to the splitting of electronic states and forms a modified joint density of states. The absorption coefficient increases with decreasing volume of quantum dot (i.e., the radius R), and it is also proportional to joint density of states. The joint density of states for a spherical quantum dot is a function of the energy gap and takes the shape of the Dirac delta function. The larger the absorption coefficient, the smaller the size of the quantum dot.

REFERENCES

- 1. C. Kittel and P. McEuen, *Introduction to Solid State Physics* (John Wiley and Sons, New York, 2005.)
- A. I. Ekimov, Al. A. Efros, and A. A. Onuschenko, Solid State Commun. 56, 921(1985).
- 3. Al. L. Efros and A. L. Efros, Sov. Phys. Semicond. **16**, 772 (1982).
- 4. Y. Kayanuma, Phys. Rev. B. 38, 9797 (1988).
- 5. L. E. Brus, J. Phys. Chem. 90, 2555 (1986).
- 6. A. Henglein, Chem. Rev. 89, 1861 (1989).
- Y. Wang, S. Suna, W. Mahler, and R. Kasowski, J. Chem. Phys. 87, 7315 (1987).
- H. Li, W. Y. Shih, and W. H. Shih, Nanotechnology 18, 205604 (2007).
- 9. C. Vatankhah and A. Edadi, Res. J. Recent Sci. 2, 21 (2013).

- 10. M. D. Ben, R. W. A. Havenith, R. Broer, and M. Stener, J. Phys. Chem. C. **115**, 16782 (2011).
- 11. A. A. A. de Queiroz, M. Martins, D. A. W. Soares, and E. J. Franca, J. Mol. Struct. **873**, 121 (2008).
- P. Coe, A. Sudbery, and I. D'Amico, Microelectron. J. 40, 499 (2009).
- 13. T. Inerbaev, A. Masunov, S. I. Khondaker, et al., J. Chem. Phys. **131**, 044106 (2009).
- 14. P. Sorokin, P. Avramov, L. A. Chernozatoskii, et al., J. Phys. Chem. **112** (40), 9955 (2008).
- S. S. Rink, D. S. Chemla, and D. A. B. Miller, J. Adv. Phys. 38, 89 (1989).
- 16. S. Schmitt-Rink, D. A. B. Miller, and D. S. Chemla, Phys. Rev. B **35**, 8113 (1987).
- 17. S. L. Chuang, *Physics of Optoelectronic Devices* (John Wiley and Sons, New York, 1995).
- 18. Sh. Khadka, *Increased Bandwidth for Dielectric Spectroscopy of Proteins through Electrode Surface Preparation. Ph. D. Thesis* (University of Illinois, Urbana-Champaign, IL, 2013).
- 19. T. S. Moss, Proc. Phys. Soc., London, Sect. B **63**, 167 (1950).
- 20. T. S. Moss, Phys. Status Solidi B 131, 415 (1985).
- 21. V. P. Gupta and N. M. Ravindra, Phys. Status Solidi B **100**, 715 (1980).
- S. Zh. Karazhanov, P. Ravindran, A. Kjekshus, et al., Phys. Rev. B. 75, 155104 (2007).